Self-Propagating High-Temperature Synthesis
Самораспространяющийся высокотемпературный синтез

UDC 621.762

https://doi.org/10.17073/1997-308X-2023-3-14-21

Research article
Научная статья

Thermal explosions in (Ti, Zr, Hf, Nb, Ta) carbon mixtures

S. G. Vadchenko[1], A. S. Sedegov[2], I. D. Kovalev[1]

[1] Merzhanov Institute of Structural Macrokinetics and Materials Science of the Russian Academy of Sciences
8 Akademik Osipyan Str., Chernogolovka, Moscow region 142432, Russia
[2] National University of Science and Technology "MISIS"
4 bld. 1 Leninskiy Prosp., Moscow 119049, Russia

vadchenko@ism.ac.ru

Abstract. This research focuses on investigating the ignition and thermal explosion behavior of (Ti, Zr, Hf, Nb, Ta) + 5C mixtures that have been mechanically activated. First, we mechanically activated the metal powder mixtures to produce composite particles consisting of Ti, Zr, Hf, Nb, and Ta, followed by the addition of carbon, and re-activation. An activation time of 120 min at 347 rpm resulted in the formation of solid solutions from the metals in the mixture, while large tantalum particles were preserved. The resulting mixtures were then pressed into pellets, which were heated in argon until ignition occurred. The ignition process involves multiple phases, with the first being inert heating, followed by progressive heating at $t = 420 \div 450$ °C, and a subsequent endothermic phase transformation at 750–770 °C. The temperature then rises rapidly, resulting in a thermal explosion that forms complex carbides, leaving some unreacted tantalum behind. The (Ti, Zr, Hf, Nb, Ta)C_5 activated mixtures and high entropy solid solution are unstable and release titanium and zirconium carbides when heated above 1300 °C, causing changes to the composition of the (Ti, Zr, Hf, Nb, Ta)C_5 final product. When diluted by adding 25 and 50 % of the final product, the effective activation energy E_a for the (Ti, Zr, Hf, Nb, Ta) + 5C reaction in the 1100–1580 °C temperature range was found to be 34 kJ/mol.

Keywords: high-entropy alloys, high-entropy carbides, ceramics, mechanical activation, thermal explosion

For citation: Vadchenko S.G., Sedegov A.S., Kovalev I.D. Thermal explosions in (Ti, Zr, Hf, Nb, Ta) carbon mixtures. *Powder Metallurgy and Functional Coatings*. 2023;17(3):14–21. https://doi.org/10.17073/1997-308X-2023-3-14-21

Тепловой взрыв в смесях (Ti, Zr, Hf, Nb, Ta) с углеродом

С. Г. Вадченко[1], А. С. Седегов[2], И. Д. Ковалев[1]

[1] Институт структурной макрокинетики и проблем материаловедения им. А.Г. Мержанова РАН
Россия, 142432, Московская обл., г. Черноголовка, ул. Акад. Осипьяна, 8
[2] Национальный исследовательский технологический университет «МИСИС»
Россия, 119049, г. Москва, Ленинский пр-т, 4, стр. 1

vadchenko@ism.ac.ru

Аннотация. В работе исследованы закономерности воспламенения и теплового взрыва механически активированных смесей (Ti, Zr, Hf, Nb, Ta) + 5C. Их готовили в 2 этапа – вначале проводили механическую активацию смесей порошков металлов для получения композитных частиц Ti, Zr, Hf, Nb, Ta, затем добавляли углерод и проводили дополнительную активацию. При активации в течение 120 мин при скорости вращения барабанов 347 об/мин формировались твердые растворы на основе входящих в состав металлов и оставались крупные частицы тантала. Из полученных смесей прессовали таблетки, которые нагревали в атмосфере аргона до воспламенения. Процесс воспламенения включает в себя несколько стадий. На первой стадии происходит инертный нагрев. При $t = 420 \div 450$ °C начинается прогрессивный разогрев образца до температур 750–770 °C, при которых происходит фазовый переход, сопровождающийся эндотермическим эффектом. После фазового перехода температура резко повышается, и происходит тепловой взрыв, в результате чего формируются сложные карбиды и остается непрореагировавший тантал. Активированная смесь и высокоэнтропийный твердый раствор

(Ti, Zr, Hf, Nb, Ta)C_5 нестабильны, и при нагреве выше 1300 °C из них выделяются карбиды. При этом изменяется состав твердого раствора (Ti, Zr, Hf, Nb, Ta)C_5. С использованием последнего для разбавления активированной смеси на 25 % и 50 % для реакции (Ti, Zr, Hf, Nb, Ta) + 5C в интервале температур 1100–1580 °C была определена эффективная энергия активации E_a = 34 кДж/моль.

Ключевые слова: высокоэнтропийные сплавы, высокоэнтропийные карбиды, керамика, механическое активирование, тепловой взрыв

Для цитирования: Вадченко С.Г., Седегов А.С., Ковалев И.Д. Тепловой взрыв в смесях (Ti, Zr, Hf, Nb, Ta) с углеродом. *Известия вузов. Порошковая металлургия и функциональные покрытия*. 2023;17(3):14–21.
https://doi.org/10.17073/1997-308X-2023-3-14-21

Introduction

Since 2004, high-entropy alloys (HEA) and high-entropy ceramics based on oxides, borides, carbides, nitrides, and hydrides have been subject of intensive research [1]. Among these materials, high-entropic carbides (HEC) have received particular attention due to their unique features [1–3]. Specifically, Ti, Zr, Hf, Nb and Ta-based HECs form stable monophase compound [4–7] with exceptional mechanical properties [8–11], low thermal conductivity [12], good oxidation resistance [13–15] and biocompatibility [16; 17].

To date, more than 20 manufacturing processes for high-entropy alloys have been developed [1]. Among the most common processes are mechanical activation (MA), spark plasma sintering (SPS), reduction from oxides, and hot pressing. Additionally, self-propagating high-temperature synthesis (SHS) can be utilized to produced HEAs by exploiting the exothermic reactions between group IV–V transition metals and carbon, boron, nitrogen or silicon [18; 19]. The SHS product is typically processed using spark plasma sintering to obtain a single-phase HEC. Although SHS is a rapid and advantageous process, the thermal explosion and combustion of HEC multicomponent mixtures have not been extensively studied.

The aim of this study is to examine the kinetics and product formation during a thermal explosion in (Ti, Zr, Hf, Nb, Ta) + C_5 mixtures.

Materials and methods

We utilized commercially available domestic powders:

– hafnium (Hf), GFM-1 grade (TU 48-4-176-85 Specs), 99.1 % purity, 180 μm average particle size;

– tantalum (Ta), TaP-1 grade (TU 1870-258-00196109-01 Specs), 99.9 % purity, d = 40÷63 μm;

– titanium (Ti), PTM-1 grade (TU 14-22-57-92 Specs), 99.2 % purity, d = 5÷15 μm;

– niobium (Nb), NbP-1a grade (GOST 26252-84), 99.7 % purity, d < 63 μm;

– zirconium (Zr), PCrK-1 grade, (TU 48-4-234-84 Specs), 99.6% purity, d = 40÷63 μm;

– graphite powder, (GOST 23463-79), 99.9999 % purity, ASC 8–4, $d \leq 140$ μm.

Activation and ignition occurred in argon of 99.998 % purity. The powder mixture was prepared in two stages. In the first stage, an equimolar mixture of Ta + Ti + Nb + Zr + Hf was activated in an Activator 2S planetary mill (Activator, Novosibirsk, Russia). The mixture was placed in pre-vacuumed steel drums and subsequently filled with argon at 6 atm. The ball-to-powder weight ratio was 1:18, with a ball weight of 360 g (5–7 mm diameter) and powder weight of 20 g. The drum rpm was 347 and the milling time was 120 min, resulting in the production of a metallic composite.

To prevent oxidation and self-ignition, the composite powder was unloaded in an argon-filled glove box. Graphite powder was added to the mixture inside the glove box to create (Ti, Zr, Hf, Nb, Ta)C_5. The resulting mixture was similarly activated for 60 min and then passivated. The drum was open for 1–2 s to allow air in, then closed and held for 10–12 h. To obtain a homogeneous mixture with the (Ti, Zr, Hf, Nb, Ta)C_5 high-entropy alloy made by SHS, a portion of the composite/graphite powder was stirred in a porcelain mortar for 30 min. The final product concentrations in these mixtures were 25 and 50 %. Samples, measuring 3 mm in diameter and up to 1.0–1.5 mm in height, were pressed from the mixtures.

The procedure for the ignition temperature test is depicted in Figure 1 [20]. The cylindrical samples were positiond on a flat thermocouple that was 30 μm thick, and then placed into either a boron nitride or graphite crucible. The crucible was subsequently placed on an electric graphite strip heater and heated to the ignition or melting temperature. The accuracy of temperature measurement was validated using the Zn, Al and Cu melting points as a reference. The margin of error at $t \leq 1100$ °C was no more than ±10 °C. The thermocouple readings were recorded at 1 kHz.

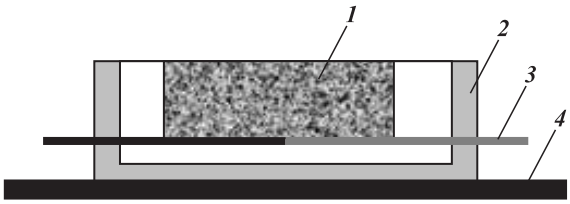

Fig. 1. Sample ignition temperature measurements
1 – sample, ***2*** – crucible, ***3*** – thermocouple, ***4*** – graphite strip heater

Рис. 1. Схема измерения температуры воспламенения образцов
1 – образец, ***2*** – тигель, ***3*** – термопара, ***4*** – графитовый ленточный нагреватель

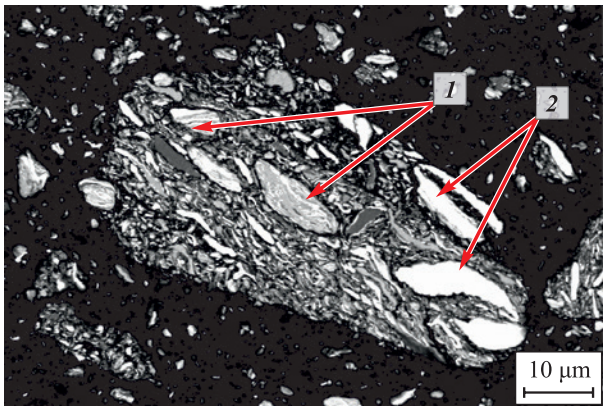

Fig. 2. Microstructure of a (Ti, Zr, Hf, Nb, Ta) mixture particle after activation and passivation
1 – layered inclusions, ***2*** – tantalum particles

Рис. 2. Микроструктура частицы смеси (Ti, Zr, Hf, Nb, Ta) после активации и пассивации
1 – слоистые включения, ***2*** – частицы тантала

For XRD of the initial samples and products after ignition, we employed a DROn 3M diffractometer with CuK_α-radiation (Burevestnik, St. Petersburg, Russia). Furthermore, we used an LEO 1450 VP microscope (Carl Zeiss, Germany) for canning electron microscopy (SEM).

Results and discussion

Figure 2 depicts the thin section microstructure of the initial Ti, Zr, Hf, Nb, and Ta composite particles. It was not possible to produce homogeneous composite particles from the metal powder mixture, as the particles contained both layered inclusions (*1*) and individual large tantalum particles (*2*).

Due to insufficient probe positioning accuracy, it was not possible to analyze smaller particles and layers. However, the SEM analysis indicated that they included all of the original elements. XRD analysis (Figure 3) indicated that the metal peaks had shifted to the left, indicating the formation of solid solutions. The tantalum and niobium peaks were nearly identical. The small peak located at approximately 40° was close to the 100 % titanium peak. Ti was found to form solid solutions with tantalum, niobium, hafnium and zirconium.

The formation of solid solutions was confirmed by the plateau observed in the thermal curves at various heating rates (V) during the initial stage ($t < 450$ °C), as shown in Figure 4. A thermal curve of the heating of the titanium sample was also included for comparison.

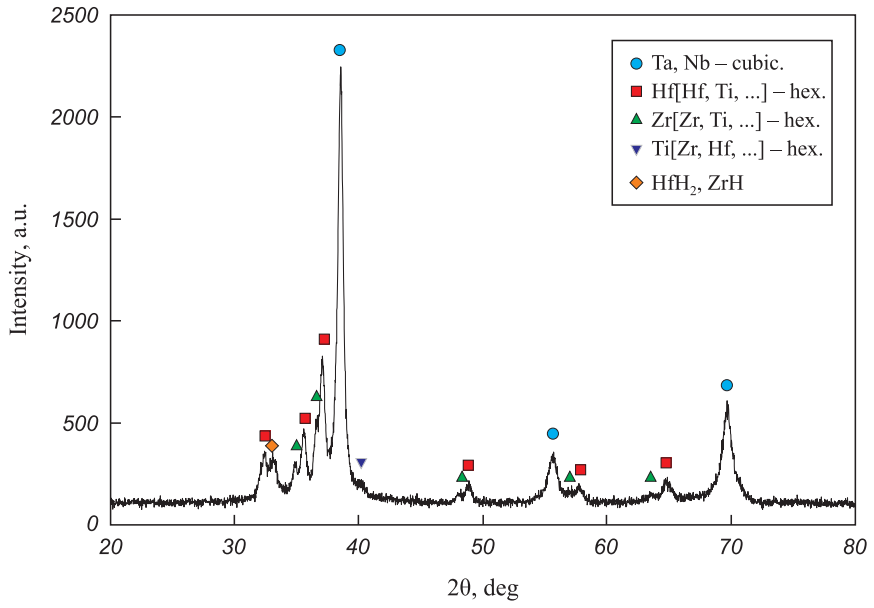

Fig. 3. XRD image of the (Ti, Zr, Hf, Nb, Ta) + 5C mixture after activation and passivation

Рис. 3. Рентгенограмма смеси (Ti, Zr, Hf, Nb, Ta) + 5C после процессов активации и пассивации

The ignition temperature (t_{ig}) at high heating rates is 1030 °C. The temperature decreases with the heating rate down to 760 °C. The thermal curves suggest that this decrease is due to a phase transformation with a significant endothermic effect, resulting in an isothermal segment in thermal curves. The α–β-transformation temperatures for titanium, zirconium, and hafnium in the Group IV metals in the mixture are $t_{\alpha-\beta}$ = 882, 865 and 1743 °C, respectively. These temperatures are considerably higher than those indicated on the thermal curves. It should be noted that the formation of solid solutions during mechanical activation can lead to a decrease in the α–β-transformation temperature in titanium. Okamoto H. and Lyakishev N.P. [21; 22] reported that $t_{\alpha-\beta}$ for titanium-zirconium equiatomic solid solutions can drop to 560–600 °C. Polymorphic transformations in Ti–Nb metastable solid solutions can occur at t = 425÷600 °C [23].

Polymorphic transformation generally enhances diffusion coefficients. This, in turn, accelerates the reaction between the solid solutions and carbon and $t_{\alpha-\beta}$ become the critical temperature of thermal explosion (t_c). The sample heating rates at the initial stage (V_1) and after ignition (V_2) were recorded as follows:

t_c, °C	760	760	770	790	830	1000
V_1, °C/s	45	47	53	68	95	240
V_2, °C/s	4250	5400	9400	11,300	8700	6500

It can be seen that the heating rate of the V_2 sample above the critical temperature is two orders of magnitude greater than the V_1 average heating rate at the initial heating stage (up to 450 °C), indicating a thermal explosion.

Figure 5 displays the XRD image of the thermal explosion products of the activated (Ti, Zr, Hf, Nb, Ta) + 5C mixture. The ignition is triggered by the formation of carbides or solid solutions of carbon in the metals, but it does not lead to the formation of the final product. Due to the short holding time at high temperatures and rapid cooling, some of the metals do not have sufficient time to react. Comparing the XRD images in Figure 3 and 5, it can be observed that the peak intensity ratio changes after the thermal explosion due to the formation of hafnium and niobium carbides.

To investigate the reaction kinetics in this system, we diluted the initial mixture with the (Ta, Ti, Nb, Zr, Hf)C_5 final product obtained by SHS. Figure 6 illustrates the thermal curves for the samples containing 25 and 50 % of the final product.

Figure 7 shows the XRD images of the products obtained by adding 25 and 50 % of the final product to the (Ti, Zr, Hf, Nb, Ta) + 5C activated mixture, and the XRD image of the final product.

The XRD images of the products obtained by heating the diluted mixture are nearly identical. The main phase formed by dilution retains its cubic lattice, but the lattice parameters differ. The XRD images reveal peaks of titanium and zirconium carbide. The XRD images of the activated mixture (see Figure 3) exhibit weakly pronounced titanium and zirconium peaks. When heated

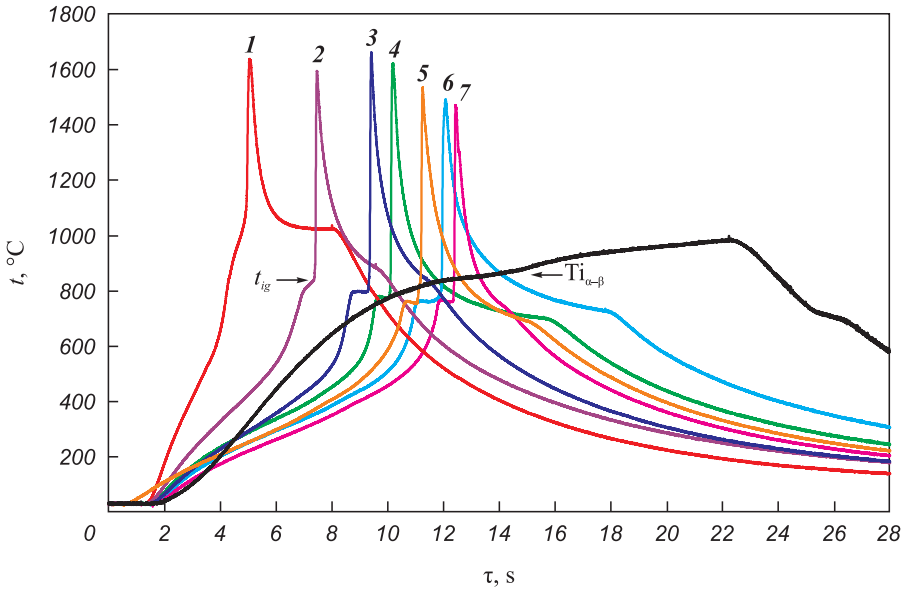

Fig. 4. Thermal curves for various heating rates of the (Ti, Zr. Hf, Nb, Ta) + 5C mixture and titanium samples
V, °C/s: 240 (***1***), 95 (***2***), 72 (***3***), 68 (***4***), 53 (***5***), 47 (***6***) and 45 (***7***)

Рис. 4. Термограммы при различных скоростях нагрева образцов из смеси (Ti, Zr. Hf, Nb, Ta) + 5C и образца из титана
V, °C/c: 240 (***1***), 95 (***2***), 72 (***3***), 68 (***4***), 53 (***5***), 47 (***6***) и 45 (***7***)

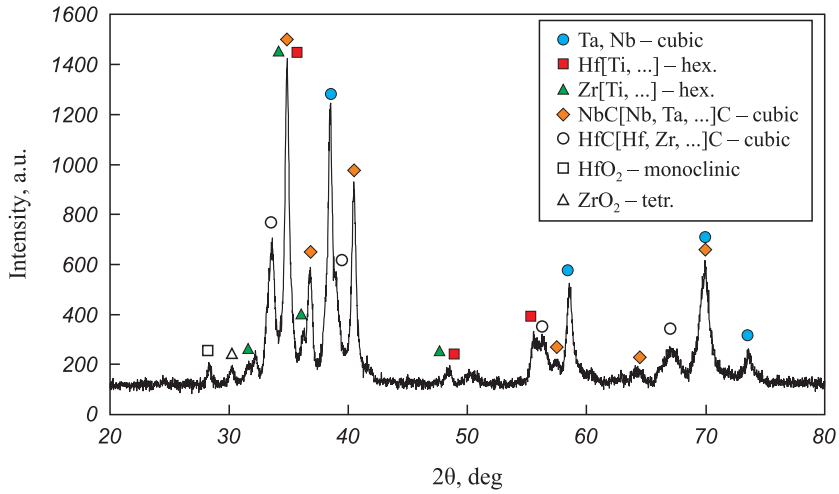

Fig. 5. XRD image of the thermal explosion products of the activated (Ti, Zr, Hf, Nb, Ta) + 5C mixture

Рис. 5. Рентгенограмма продуктов теплового взрыва активированной смеси (Ti, Zr, Hf, Nb, Ta) + 5C

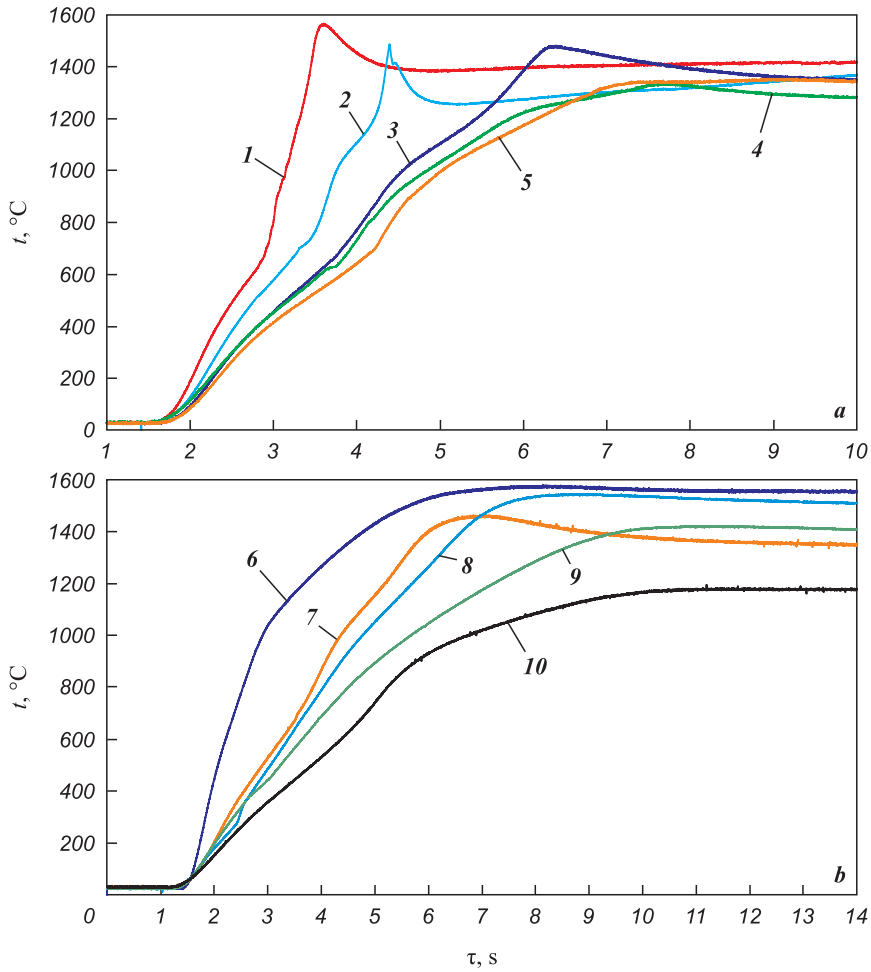

Fig. 6. Thermal curves for various heating rates of the (Ti, Zr, Hf, Nb, Ta) + 5C mixtures containing 25 (***a***) and 50 % (***b***) of the (Ti, Zr, Hf, Nb, Ta)C_5 final product
a – V = 550 °C/s (***1***), 480 (***2***), 310 (***3***), 280 (***4***) and 140 (***5***)
b – V = 730 °C/s (***6***), 340 (***7***), 310 (***8***), 295 (***9***) and 190 (***10***)

Рис. 6. Термограммы при различных скоростях нагрева образцов из смесей (Ti, Zr, Hf, Nb, Ta) + 5C, содержащих 25 (***a***) и 50 % (***b***) конечного продукта (Ti, Zr, Hf, Nb, Ta)C_5
a – V = 550 °C/c (***1***), 480 (***2***), 310 (***3***), 280 (***4***) и 140 (***5***)
b – V = 730 °C/c (***6***), 340 (***7***), 310 (***8***), 295 (***9***) и 190 (***10***)

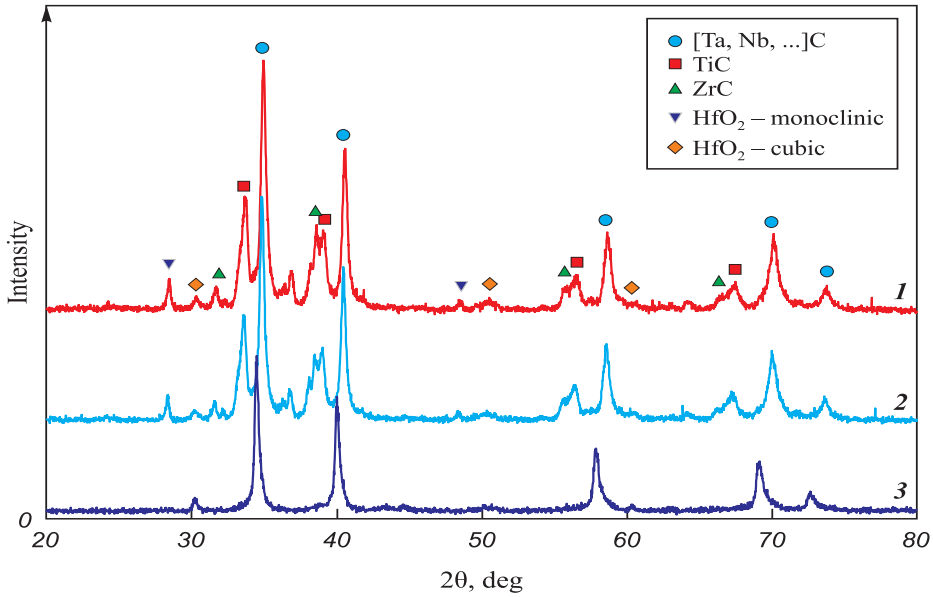

Fig. 7. XRD images of the products obtained by heating the activated (Ti, Zr, Hf, Nb, Ta) + 5C mixture diluted by 25 % (***1***) and 50 % (***2***) of the (Ti, Zr, Hf, Nb, Ta)C_5 final product (***3***)

Рис. 7. Рентгенограммы продуктов нагрева активированной смеси (Ti, Zr, Hf, Nb, Ta) + 5C, разбавленной на 25 % (***1***) и 50 % (***2***), и конечного продукта (Ti, Zr, Hf, Nb, Ta)C_5 (***3***)

above 1300 °C, the peaks of Ti and Zr carbide become visible. We can conclude that the solid solutions formed after activation and the dilution of high-entropy phase are unstable at high temperatures (t > 1300 °C), resulting in the release of titanium and zirconium carbides. The composition of the (Ti, Zr, Hf, Nb, Ta)C_5 high-entropy phase also changes.

Since the compositions of the ignition products of the diluted mixture are nearly identical, we used the max temperature vs. heating rate curves for the two dilutions to estimate the activation energy using the Kissinger equation. The reaction rate in the diluted mixtures decreased significantly, and the sample overheating was low. Furthermore, the temperature gradient across the relatively thin samples (about 1 mm thick) was insignificant. Considering these factors, we estimated the activation energy for the reaction forming the (Ti, Zr, Hf, Nb, Ta)C_5 high-entropic phase as follows:

$$\ln\left(\frac{\beta}{T_{max}^2}\right) = \ln\left(\frac{AR}{E_a}\right) - \frac{E_a}{RT_{max}},$$

where β is the heating rate, degrees/s; E_a is the activation energy, kJ/mol; R = 8.314 J/(mol·K) is the gas constant; A is the pre-exponential factor of the Arrhenius equation (particle collision frequency, s^{-1}); T_{max} is the max temperature, K.

Figure 8 shows the $\ln\left(\frac{\beta}{T_{max}^2}\right)$ vs. T_{max}^{-1} curve.

The activation energy E_a for the reaction of the (Ti, Zr, Hf, Nb, Ta) + 5C activated mixtures diluted with the final product in the temperature range of 1100–1580 °C, was found to be 34 kJ/mol. This value is significantly lower, by 75–80 %, than the value estimated from previous experimental data on gasless combustion of metal-carbon systems [24]. One possible explanation for this discrepancy is that the mechanical activation process resulted in an increase in the reactivity of the metals, which may be attributed to the grinding

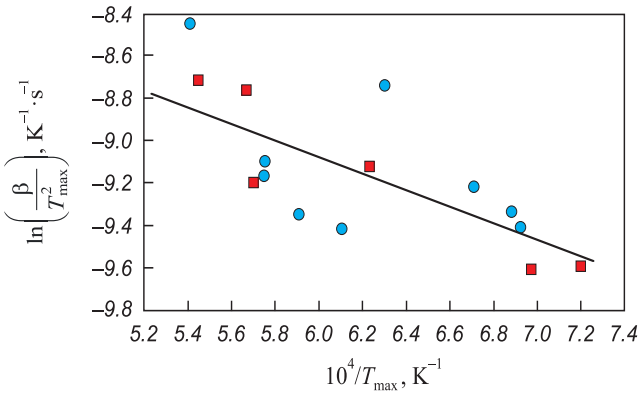

Fig. 8. The reaction activation energy estimated with Kissinger's equation
The activated mixtures (Ti, Zr, Hf, Nb, Ta) + 5C are diluted by adding 25 % (■) and 50 % (●) of the final product

Рис. 8. Результаты оценки энергии активации реакции по уравнению Киссинджера
Разбавление конечным продуктом активированных смесей (Ti, Zr, Hf, Nb, Ta) + 5C на 25 % (■) и 50 % (●)

process, the closer contacts between reactants and the introduction of more crystal lattice defects.

Conclusions

1. The mechanical activation of (Ti, Zr, Hf, Nb, Ta) + 5C mixtures for 120 min at 347 rpm produces composite particles and solid solutions of Ti, Zr, Hf, Nb and Ta, while individual tantalum particles remain in the mixture.

2. The ignition of the (Ti, Zr, Hf, Nb, Ta) + 5C activated mixture occurs in several stages, including inert heating, progressive heating to 420–450 °C and phase transformation at 750–770 °C. A thermal explosion occurs when the temperature raises abruptly.

3. Despite the high temperatures, the reaction produces complex carbides, and unreacted tantalum remains due to the short duration of the thermal explosion.

4. The activated mixtures and high entropy solid solution are unstable. When heated above 1300 °C, they release titanium and zirconium carbides. This process also causes a change in the composition of the (Ti, Zr, Hf, Nb, Ta)C_5 final product.

5. The effective activation energy estimated for the reaction in the (Ti, Zr, Hf, Nb, Ta) + 5C mixture (E_a = 34 kJ/mol) is 75–80 % lower than the values reported for the metal + carbon combustion reactions. This could be attributed to the mechanical activation of the mixture.

References / Список литературы

1. Akrami S., Edalati P., Fuji M., Edalati K. High-entropy ceramics: Review of principles, production and applications. *Materials Science and Engineering: R: Reports*. 2021;146:100644. https://doi.org/10.1016/j.mser.2021.100644
2. Ye B., Wen T., Huang K., Wang C.Z., Chu Y. First-principles study, fabrication, and characterization of ($Hf_{0.2}Zr_{0.2}Ta_{0.2}Nb_{0.2}Ti_{0.2}$)C high-entropy ceramic. *Journal of the American Ceramic Society*. 2019;102(7):4344–4352. https://doi.org/10.1111/jace.16295
3. Zhang Q., Zhang J., Li N., Chen W. Understanding the electronic structure, mechanical properties, and thermodynamic stability of (TiZrHfNbTa)C combined experiments and first-principles simulation. *Journal of Applied Physics*. 2019;126(2):025101. https://doi.org/10.1063/1.5094580
4. Kochetov N.A., Kovalev I.D. Synthesis and thermal stability of the multielement carbide (TaZrHfNbTi)C_5. *Inorganic Materials*. 2021:57(1):8–13. https://doi.org/10.1134/S0020168520120109
5. Kovalev D.Yu., Kochetov N.A., Chuev I.I. Fabrication of high-entropy carbide (TiZrHfTaNb)C by high-energy ball milling. *Ceramics International*. 2021;47(23):32626–32633. https://doi.org/10.1016/j.ceramint.2021.08.158
6. Sarker P., Harrington T.J., Gild J., Sarker P., Toher C., Rost C.M., Dippo O.F., McElfresh C., Kaufmann K., Marin E., Borowski L., Hopkins P.E., Luo J., Curtarolo S., Brenner D.W., Vecchio K.S. Phase stability and mechanical properties of novel high entropy transition metal carbides. *Acta Materialia*. 2019;166:271–280. https://doi.org/10.1016/j.actamat.2018.12.054
7. Sarker P., Harrington T.J., Toher C., Oses C., Samiee M., Maria J.P., Brenner D.W., Vecchio K.S., Curtarolo S. High-entropy high-hardness metal carbides discovered by entropy descriptors. *Nature Communications*. 2018;9:4980. https://doi.org/10.1038/s41467-018-07160-7
8. Jiang S., Shao L., Fan T., Duan J.M., Chen X.T., Tang B.Y. Mechanical behavior of high entropy carbide (HfTaZrTi)C and (HfTaZrNb)C under high pressure: Ab initio study. *International Journal of Quantum Chemistry*. 2020;121(5): 1–11. https://doi.org/10.1002/qua.26509
9. Moskovskikh D.O., Vorotilo S., Sedegov A.S., Kuskov K.V., Bardasova K.V., Kiryukhantsev-Korneev Ph.V., Zhukovskyi M., Mukasyan A.S. High-entropy (HfTaTiNbZr)C and (HfTaTiNbMo)C carbides fabricated through reactive high-energy ball milling and spark plasma sintering. *Ceramics International*. 2020;46(11B):19008–19014. https://doi.org/10.1016/j.ceramint.2020.04.230
10. Wang F., Zhang X., Yan X., Lu Y., Nastasi M., Chen Y., Cui B. The effect of submicron grain size on thermal stability and mechanical properties of high-entropy carbide ceramics. *Journal of the American Ceramic Society*. 2020;103(8):4463–4472. https://doi.org/10.1111/jace.17103
11. Feng L., Fahrenholtz W.G., Hilmas G.E. Low-temperature sintering of single-phase, high-entropy carbide ceramics. *Journal of the American Ceramic Society*. 2019;102(12):7217–7224. https://doi.org/10.1111/jace.16672
12. Chen H., Xiang H., Dai F.Z., Liu J., Lei Y., Zhang J., Zhou Y. High porosity and low thermal conductivity high entropy ($Zr_{0.2}Hf_{0.2}Ti_{0.2}Nb_{0.2}Ta_{0.2}$)C. *Journal of Materials Science & Technology*. 2019;35(8):1700–1705. https://doi.org/10.1016/j.jmst.2019.04.006
13. Ye B., Wen T., Liu D., Chu Y. Oxidation behavior of ($Hf_{0.2}Zr_{0.2}Ta_{0.2}Nb_{0.2}Ti_{0.2}$)C high-entropy ceramics at 1073–1473 K in air. *Corrosion Science*. 2019;153: 327–332. https://doi.org/10.1016/j.corsci.2019.04.001
14. Ye B., Wen T., Chu Y. High-temperature oxidation behavior of $Hf_{0.2}Zr_{0.2}Ta_{0.2}Nb_{0.2}Ti_{0.2}$)C high-entropy ceramics in air. *Journal of the American Ceramic Society*. 2020;103(1):500–507. https://doi.org/10.1111/jace.16725
15. Wang H., Cao Y., Liu W., Wang Y. Oxidation behavior of ($Hf_{0.2}Ta_{0.2}Zr_{0.2}Ti_{0.2}Nb_{0.2}$)C-xSiC ceramics at high temperature. *Ceramics International*. 2020;46(8A):11160–11168. https://doi.org/10.1016/j.ceramint.2020.01.137
16. Braic V., Vladescu A., Balaceanu M., Luculescu C.R., Braic M. Nanostructured multi-element (TiZrNbHfTa)N and (TiZrNbHfTa)C hard coatings. *Surface and Coatings Technology*. 2012;211:117–121. https://doi.org/10.1016/j.surfcoat.2011.09.033
17. Braic V., Balaceanu M., Braic M., Vladescu A., Panseri S., Russo A. Characterization of multiprincipal-element (TiZrNbHfTa)N and (TiZrNbHfTa)C coatings for biomedical applications. *Journal of the Mechanical Be-*

havior of Biomedical Materials. 2012;10:197–205. https://doi.org/10.1016/j.jmbbm.2012.02.020

18. Merzhanov A.G., Borovinskaya I.P. Self-propagated high-temperature synthesis of refractory inorganic compounds. *Doklady Chemistry Proceedings of the Academy of Sciences of the USSR. Chemistry Section*. 1972;204(2):429–433.
19. Tallarita G., Licheri R., Garroni S., Orrù R., Cao G. Novel processing route for the fabrication of bulk high-entropy metal diborides. *Scripta Materialia*. 2019;158:100–104. https://doi.org/10.1016/j.scriptamat.2018.08.039
20. Vadchenko S.G., Boyarchenko O.D., Shkodich N.F., Rogachev A.S. Thermal explosion in various Ni–Al systems: Effect of mechanical activation. *International Journal of Self-Propagating High-Temperature Synthesis*. 2013;22(1):60–64. https://doi.org/10.3103/S1061386213010123
21. Okamoto H. Desk handbook: Phase diagrams for binary alloys. 2nd Ed. Edited by ASM International Materials Park. Ohio, USA. 2010. 855 p.
22. Lyakishev N.P. (Ed.) Dual metal system state diagrams: Reference book. In 3 volumes. Vol. 1. Moscow: Mashinostroenie, 1996. 992 p. (In Russ.).

    Диаграммы состояния двойных металлических систем: Справочник. В 3 т. Т. 1. Под общ. ред. Н.П. Лякишева. М.: Машиностроение, 1996. 992 с.
23. Zhang Y., Liu H., Jin Z. Thermodynamic assessment of the Nb–Ti system. *Calphad*. 2001;25(2):305–317. https://doi.org/10.1016/S0364-5916(01)00051-7
24. Mukasyan A.S., Rogachev A.S. Discrete reaction waves: Gasless combustion of solid powder mixtures. *Progress in Energy and Combustion Science*. 2008;34(3):377–416. https://doi.org/10.1016/j.pecs.2007.09.002
25. Egorychev K.N., Kurbatkina V.V., Levashov E.A. Prospects for the use of mechanical activation of low-exothermal materials for synthesis of composite materials by SHS technology. *Izvestiya vuzov. Tsvetnaya metallurgiya*. 1996;(6):49–52. (In Russ.).

    Егорычев К.Н., Курбаткина В.В., Левашов Е.А. Перспективы применения механического активирования низкоэкзотермических материалов для синтеза композиционных материалов СВС-технологией. *Известия вузов. Цветная металлургия*. 1996;(6):49–52.
26. Korchagin M.A. Thermal explosion in mechanically activated low-calorie compositions. *Fizika goreniya i vzryva*. 2015;51(5):77–86. (In Russ.). http://dx.doi.org/10.15372/FGV20150509

    Корчагин М.А. Тепловой взрыв в механически активированных низкокалорийных составах. *Физика горения и взрыва*. 2015;51(5):77–86. http://dx.doi.org/10.15372/FGV20150509

Information about the Authors

Sergey G. Vadchenko – Cand. Sci. (Phys.-Math.), Leading Researcher, Microheterogenic Process Dynamics Laboratory, Merzhanov Institute of Structural Macrokinetics and Materials Science, Russian Academy of Sciences.
ORCID: 0000-0002-2360-2114
E-mail: vadchenko@ism.ac.ru

Aleksei S. Sedegov – Engineer, Structural Nanoceramics Research Center, National University of Science and Technology "MISIS"
ORCID: 0000-0002-4927-8930
E-mail: a.sedegov@misis.ru

Ivan D. Kovalev – Cand. Sci. (Phys.-Math.), Senior Researcher, *X*-Ray Structural Research Laboratory, Merzhanov Institute of Structural Macrokinetics and Materials Science, Russian Academy of Sciences.
ORCID: 0000-0003-4710-837X
E-mail: i2212@yandex.ru

Сведения об авторах

Сергей Георгиевич Вадченко – к.ф.-м.н., вед. науч. сотрудник лаборатории динамики микрогетерогенных процессов, Институт структурной макрокинетики и проблем материаловедения им. А.Г. Мержанова Российской академии наук (ИСМАН).
ORCID: 0000-0002-2360-2114
E-mail: vadchenko@ism.ac.ru

Алексей Сергеевич Седегов – инженер НИЦ «Конструкционные керамические наноматериалы», Национальный исследовательский технологический университет «МИСИС».
ORCID: 0000-0002-4927-8930
E-mail: a.sedegov@misis.ru

Иван Дмитриевич Ковалев – к.ф.-м.н., ст. науч. сотрудник лаборатории рентгеноструктурных исследований, ИСМАН.
ORCID: 0000-0003-4710-837X
E-mail: i2212@yandex.ru

Contribution of the Authors

S. G. Vadchenko – problem statement, tests, text authoring.

A. S. Sedegov – mixture and sample preparation, discussion.

I. D. Kovalev – XRD analysis, discussion.

Вклад авторов

С. Г. Вадченко – определение целей работы, проведение экспериментов, написание текста статьи.
А. С. Седегов – подготовка смесей и исходных образцов, участие в обсуждении результатов.
И. Д. Ковалев – проведение рентгенофазового анализа, участие в обсуждении результатов.

Received 22.06.2022
Revised 11.11.2022
Accepted 19.12.2022

Статья поступила 22.06.2022 г.
Доработана 11.11.2022 г.
Принята к публикации 19.12.2022 г.